Buffer-Layer-Assisted Growth of Nanocrystals: Ag-Xe-Si(111)

Lin Huang, S. Jay Chey, and J. H. Weaver

Department of Materials Science and Chemical Engineering, University of Minnesota, Minneapolis, Minnesota 55455

(Received 10 November 1997)

Silver nanocrystals have been grown on Xe buffer layers at 50 K. These 3D nanocrystals are delivered to Si(111)-(7 × 7) surfaces when the Xe layer is desorbed, but the density observed on the surface depends strongly on the buffer layer thickness. This dependence reflects an unusual desorption-assisted coalescence process. The results suggest that buffer-layer-assisted growth can be used to prepare nanocrystals of different sizes for a wide variety of materials and substrates. [S0031-9007(98)05945-6]

PACS numbers: 81.10.–h, 61.16.Ch, 61.46.+w

Considerable effort is being expended to develop specific solid state structures with nanoscopic dimension(s), as in thin films, quantum wires, or quantum dots. A common thread in this work is the manipulation of the thermodynamic parameters that dictate a particular growth mode [1–3]. In quantum dots, the goal is to produce nanostructures in three dimensions [4]. The challenge for 3D growth for a given adlayer/substrate system, however, is that Volmer-Weber growth places specific constraints on the surface and interface free energies, and those systems that meet the necessary conditions are the exception rather than the rule.

In this Letter, we focus on a growth and delivery process that avoids the constraints of thermodynamics while producing clusters and nanocrystals under conditions that preserve atomic-scale cleanliness. This "buffer-layer-assisted growth" or BLAG process was developed to produce abrupt interfaces [5], but with scanning tunneling microscopy (STM), we can now report real-space visualization of the resulting structures. We demonstrate that BLAG is unlike conventional growth, because clusters form on the buffer layer and then coalesce as the buffer layer desorbs (hence desorption-assisted coalescence). Accordingly, the nanocrystal size distribution can be controlled by adjusting the thickness of the buffer layer. This growth and delivery pathway offers an opportunity to produce a wide range of nanocrystals on any desired substrate with reasonable control over the size distribution.

The key to the BLAG process is the condensation of inert buffer layers at low temperature so as to prevent subsequently deposited atoms from directly interacting with the substrate. Instead, these adatoms diffuse on the buffer layer to form 3D clusters, and buffer layer desorption brings the 3D clusters into "soft-landing" contact with the pristine substrate [6]. Here, we use Xe as the buffer layer. Nanocrystal formation on Xe can be understood because the surface free energy is extremely low [$\gamma_{\mathrm{Xe}} \cong 0.063$ J/m^2 for Xe(100)] and adatom interactions with Xe are weak, giving a low interface energy γ_i. Hence, the 3D growth condition is always satisfied, $\gamma_{\mathrm{Xe}} < \gamma_d + \gamma_i$, where γ_d is the surface free energy of deposited material [~ 0.62 J/m^2 for Ag(111)], and nucleation and growth will occur regardless of the underlying substrate.

The experiments here focus on Ag nanocrystals and Si(111)-(7 × 7) substrates, with STM used to characterize the nanocrystal size distributions after delivery to the Si surface. The measurements were performed in ultrahigh vacuum (base pressure $< 5 \times 10^{-11}$ Torr). Si(111)-(7 × 7) samples were cleaned and characterized in the measurement chamber before being transferred to a connected chamber where they were cooled to 50 K and exposed to ultrapure Xe. The layer thickness can be estimated from the Xe exposure [7]. After Xe overlayer growth, the buffered sample was exposed to a flux of Ag atoms from a thermal source (~ 0.6 Å/min). The amount of Ag is expressed in units of angstroms, where 2.36 Å represents 1 monolayer (ML) of Ag(111) but layer-by-layer growth is not implied. Thereafter, the samples were warmed and transferred to the STM for imaging at room temperature. Usually, the warm-up process was rapid as the samples were removed from the cold stage by a room-temperature transfer fork. An alternate procedure that involved warming at 2 K/min from 50 to 100 K gave similar morphologies. Atomic resolution images showed that there was no significant increase in the 7 × 7 defect density due to Xe or Ag exposure [7]. Considerable care was taken to avoid the influence of the STM tip on the stability of the nanocrystals.

Figure 1 shows representative STM images for Ag deposition of 0.2 Å onto Xe layers of ~ 4, 60, and 300 ML [8]. In contrast to the layer-by-layer growth observed for conventional Ag atom deposition onto Si(111) at a low temperature [9], we see randomly distributed 3D islands. The density of islands in Fig. 1(a) is 1.4×10^{12} cm^{-2} as deduced from large-scan images from different areas. The average center-to-center separation is ~ 85 Å. This is consistent with experiments for Ag/Xe/GaAs(110) where the sizes and densities of clusters *on the Xe layer* were estimated from photoemission attenuation results. Assuming a uniform hemispherical structure, Ref. [5] estimated

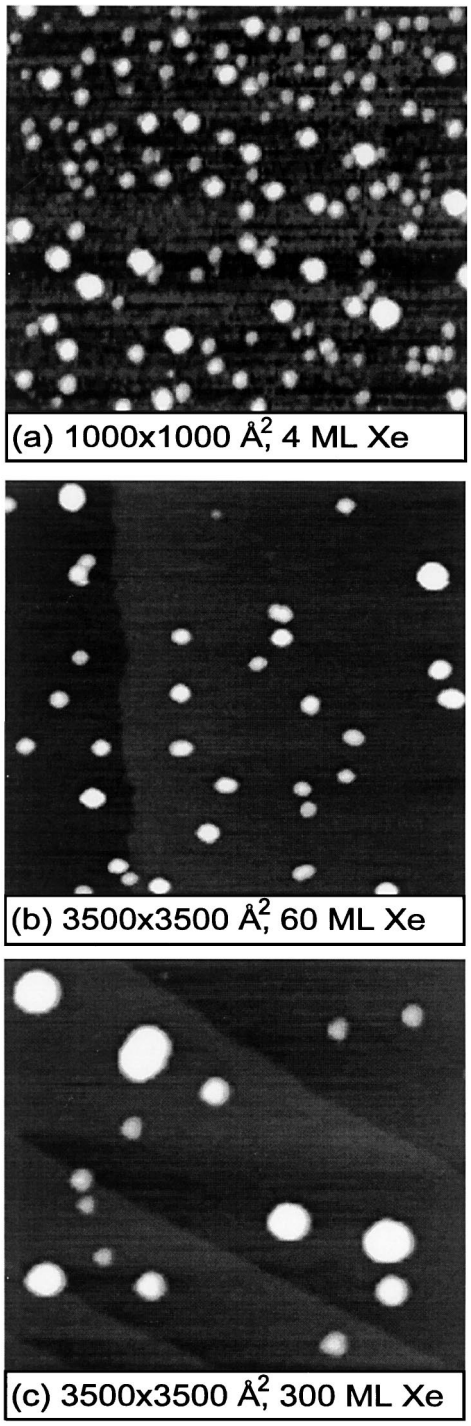

FIG. 1. Surface morphology produced when 0.2 Å Ag was deposited on Xe buffered Si(111)-(7 × 7) at 50 K and subsequently imaged at room temperature after Xe desorption. The bright features are 3D Ag islands. Their density of 1.4×10^{12} cm^{-2} in (a) represents the density of clusters "as formed" on the buffer layer. This density decreases in (b) and (c) due to desorption-assisted coalescence. The number of atoms in the large nanostructures of (c) is ~ 90 000, compared to an average of ~ 3000 in (b) and only 28 in (a).

an average cluster radius of 7 Å and a density of 6×10^{12} cm^{-2} for 0.5 Å Ag deposition.

The island density in the nucleation and growth regime is related to the diffusion coefficient of the deposited material on the surface [1]. Mo *et al.* [10] obtained a simplified relationship $N^3 = 3R\theta/D$ between the number density of stable islands, N, and the surface diffusion coefficient of monomers, D, where R is the deposition rate and θ is the total coverage. We can estimate roughly the diffusion properties of Ag on Xe with the values of Xe diffusion on Pt(111) [11], obtaining $D = 3.2 \times 10^{-8}$ cm^2 s^{-1} and $N \cong 10^{12}$ cm^{-2}. This density corresponds rather well with the STM results of Fig. 1(a) when $\theta = 0.2$ Å and $R = 0.6$ Å/min. We conclude that Fig. 1(a) approximates the nucleation and growth morphology of Ag on the thinnest effective Xe buffer layer and that the sublimation of such a layer did not significantly change the cluster size and distribution.

Remarkably, the images in Figs. 1(b) and 1(c) reveal quite different morphologies because the nanostructure density decreased to 2.6×10^{10} and 1.1×10^{10} cm^{-2} for buffer layer thicknesses of 60 and 300 ML while the amount of Ag was held fixed. Correspondingly, the average distance between Ag crystals increased to 620 and 950 Å, respectively. We can use the height, obtained from STM line scans, as an estimate of the crystal size, noting that the "footprint" of a crystal is determined less accurately with STM because of tip effects (Ref. [12]), To get an idea of the number of atoms in the crystal of Fig. 1(c), we can assume a hemispherical shape, giving 340 to 90 000 atoms. Within this approximation, we could calculate the total amount of Ag deposited, and the result was very close to the value obtained from the microbalance thickness monitor. Figure 2 summarizes the nanocrystal height distributions as a function of Xe layer thickness. The structures in Fig. 1(a) range in height from 3 to 12 Å, and the average height is ~ 6 Å. The dispersion of this distribution $s_d = (\langle h^2 \rangle - \langle h \rangle^2)^{1/2}$ is only 2 Å. Increasing the buffer layer thickness to 60 ML increased the average height to 29 Å [Fig. 1(b)] and the range from 14 to 38 Å with $s_d = 4.8$ Å. For a 300 ML thick Xe layer, there was a much wider range from 14 to 90 Å [Fig. 1(c)] and a significant increase of s_d to 18.2 Å.

To extend the above observations, we determined the density of Ag nanocrystals as a function of Ag deposition. Figure 3 shows such results for buffer layers of 4, 60, and 300 ML. While it is evident that this density depends only weakly on the amount of Ag deposited onto a buffer layer of a given thickness, the densities depend strongly on the buffer layer thickness. From classical nucleation theory [10], we calculated the density change expected as a function of Ag deposition on the Xe layer, and we fitted this to the three data points for the 4 ML buffer layer. Assuming that the dashed line reflects densities for nucleation and growth on the Xe layer, then there is a decrease in density as the clusters are delivered to the substrate. The dependence is evident in Fig. 3 when the density decreased by a factor of 260 for 0.2 Å Ag on

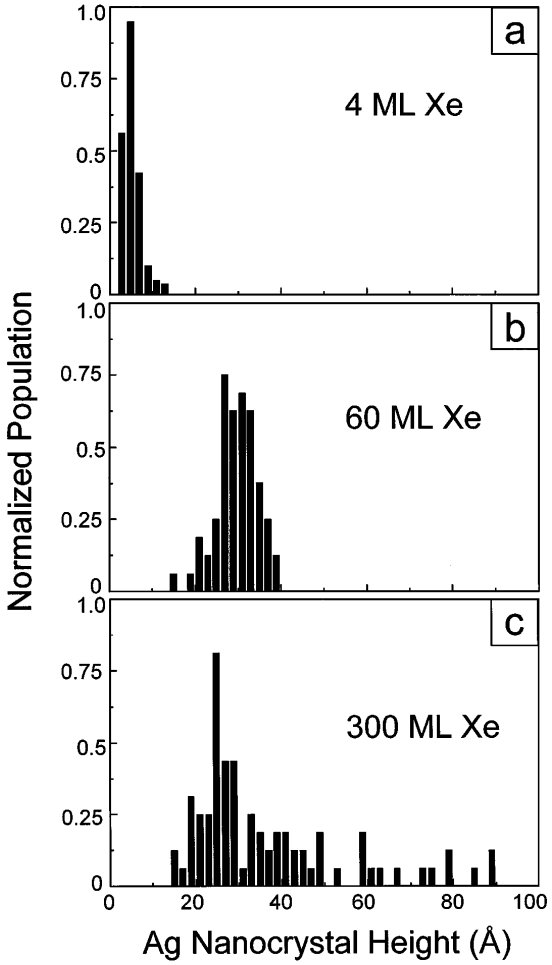

FIG. 2. Height distribution for Ag nanocrystals formed by deposition of 0.2 Å on buffer layers of different thickness. For ~4 ML Xe (a), the height range is from 3 to 12 Å but it increases to 14 to 38 Å for 60 ML Xe (b), and 14 to 90 Å for 300 ML Xe (c).

4–2000 ML Xe. The density changed abruptly between 4 and 24 ML but then the rate of changes decreased.

These results demonstrate an unusual process that we term desorption-assisted coalescence. As described below, this process is, to some extent, similar to coagulation in colloid suspensions [13]. It is also similar to the dynamic coalescence activated by temperature, mechanical vibrations, irradiation, and electrical fields for metal deposition on amorphous carbon and alkali halides [14].

The central part of desorption-assisted coalescence and these other dynamic coalescence processes is that the particles become mobile due to external perturbations, and they perform random walks. Accordingly, two particles of radii r_1 and r_2 can collide and merge into one with radius r_3 given by $r_3 = (r_1^3 + r_2^3)^{1/3}$. With increasing time, the processes of particle migration, collision, and merging result in the disappearance of small structures and growth of larger ones. This leads to an increase of both the average size and the dispersion of their size distributions. These consequences are all manifest

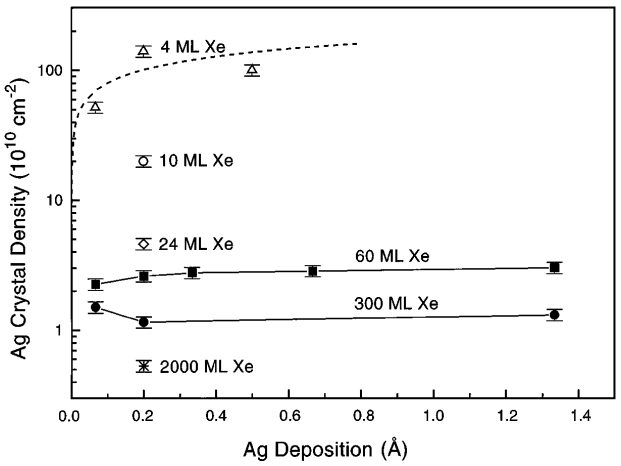

FIG. 3. Nanocrystal density as a function of Ag deposition and buffer layer thickness. For the thinnest layers (4 ML), there is little desorption-assisted coalescence, and the dashed line reflects nucleation and growth on the Xe layer. The density decreases with the layer thickness at fixed Ag deposition but is nearly constant for fixed thick Xe layer thickness.

here for Ag deposition on thick buffer layers where the desorption process represents the external perturbation.

In the STM images, we generally observe single crystallites with only occasional structures that appear to be in the process of coalescing. This indicates that the merging process is rapid compared to the diffusional time. This can be understood by noting the high cohesive energy of Ag (2.9 eV atom^{-1}) and the simplicity of the fcc structure. Hence, the rate-limiting step in desorption-assisted coalescence is diffusion. By analogy to 2D diffusion [14], the kinetics of coalescence would reflect the number of binary collisions, and this is proportional to $\delta D(r)C^n$, where δ describes the efficiency of the collision, C is the concentration, and $D(r)$ is the equivalent diffusion coefficient which depends on particle radius r. Here, $\delta = 1$ since the van der Waals forces between particles of the same material in a medium are always attractive. The exponent n falls between 2 and 3 since the clusters are not confined to a 2D substrate ($n = 2$) or distributed homogeneously within the Xe multilayer ($n = 3$).

There are many theoretical studies in 2D or 3D for dynamic coalescence and colloidal aggregation [13–15]. While the details associated with Xe desorption are not yet fully understood [16], the mechanisms of the desorption-assisted coalescence can be qualitatively understood. Sublimation is likely to start from steps and defects, or around the Ag crystallites, when the sample is warmed through the multilayer desorption temperature. Rapid desorption will induce particle movement, and those that meet will coalesce, releasing energy that will contribute to further movement. These processes will continue until the crystals land on the substrate. The thicker the Xe layer, the greater the number of collisions. At the onset of desorption-assisted coalescence, the concentration C is high and $D(r)$

is large due to the high mobility of small structures. The number of collisions is then large, and this indicates a fast process. With time, the decrease in C reduces the likelihood of encountering another crystallite, and the growing crystallites are less mobile. Considering these factors, the changes in surface morphology will be profound for thin buffer layers but the changes become more gradual as the buffer layer thickens. Experimentally, we observe that the cluster density drops abruptly with the desorption of thin multilayers of Xe (Fig. 3), but decreases slowly between 60 and 2000 ML. This behavior is similar to simulations of two dimensional cluster-cluster aggregation in the diffusion limited regime [13].

This new pathway of nanocrystal formation and delivery has several advantages. First, the interface energy and substrate effects can be eliminated, and the 3D crystals will grow. Second, a wide range of nanostructured materials can be assembled, and the choice of the substrate and its surface condition can be varied. Finally, the nanocrystal size and density can be controlled by varying the buffer layer thickness and the assembly procedure. Interesting nanostructures can be fabricated and their compatibility with other structures can be investigated. For example, preliminary measurements of the Ag BLAG process on Ag(111) show nanoscale wetting phenomena associated with delivery. Results for Ag on Si(111) show that the STM tip can be used to manipulate the nanocrystals and to "paint" with Ag atoms by site-specific adhesive wear.

This work was supported by the Office of Naval Research. The authors appreciate stimulating discussions with G. Comsa, Z. Zhang, and K. Nakayama.

[1] J. A. Venables, G. D. T. Spiller, and M. Hanbucken, Rep. Prog. Phys. **47**, 399 (1984).

[2] M. Copel, M. C. Reuter, E. Kaxiras, and R. M. Tromp, Phys. Rev. Lett. **63**, 632 (1989).

[3] R. Kunkel, B. Poelsema, L. K. Verheij, and G. Comsa, Phys. Rev. Lett. **65**, 733 (1990).

[4] D. C. Ralph, C. T. Black, and M. Tinkham, Phys. Rev. Lett. **78**, 4087 (1997).

[5] G. D. Waddill, I. M. Vitomirov, C. M. Aldao, and J. H. Weaver, Phys. Rev. Lett. **62**, 1568 (1989); G. D. Waddill, I. M. Vitomirov, C. M. Aldao, S. G. Anderson, C. Capasso, and J. H. Weaver, Phys. Rev. B **41**, 5293 (1990); J. H. Weaver and G. D. Waddill, Science **251**, 1444 (1991).

[6] K. Bromann, C. Felix, H. Brune, W. Harbich, R. Monot, J. Buttet, and K. Kern, Science **274**, 956 (1996).

[7] Correcting the ion gauge reading for its sensitivity to Xe and assuming a sticking coefficient of unity from 25 to 52 K gives a growth rate of 1 ML per 10 L exposure, where 1 ML is the atom density of Xe(111) and 1 L $= 10^{-6}$ Torr s. See J. W. Bartha, U. Barjenbruch, and M. Henzler, J. Phys. C **19**, 2459 (1986).

[8] For very thin layers, the Xe growth structure on Si(111) is not uniform [E. Conrad and M. B. Webb, Surf. Sci. **129**, 37 (1983); J. W. Bartha and M. Henzler, Surf. Sci. **160**, 379 (1985)]. Xe will initially adsorb selectively to produce a layer having an adatom density that is about half of the close-packed density. Further exposure leads to formation of noncontinuous Xe multilayers. Our results provide a way of confirming this distribution since we find clusters distributed uniformly over large areas of the surface (where the buffer layer was thick enough) but also areas where growth resembles that for low temperature conventional Ag deposition (where the buffer layer was insufficient). The lowest exposure studied corresponds to 20 L of Xe. For it, the area decorated with clusters was about 50%, and we estimate the layer thickness to be ~ 4 ML. The amount of unprotected surface decreases with Xe exposure, and uniform surface morphologies were observed for exposures exceeding 200 L (~ 20 ML).

[9] G. Meyer and K. H. Rieder, Appl. Phys. Lett. **64**, 3560 (1994).

[10] Y. W. Mo, J. Kleiner, M. B. Webb, and M. G. Lagally, Phys. Rev. Lett. **66**, 1998 (1991).

[11] E. G. Seebauer and C. E. Allen, Prog. Surf. Sci. **49**, 265 (1995).

[12] D. W. McComb, B. A. Collings, R. A. Wolkow, D. J. Moffatt, C. D. MacPherson, D. M. Rayner, P. A. Hackett, and J. E. Hulse, Chem. Phys. Lett. **251**, 8 (1996).

[13] P. Meakin, in *Phase Transitions and Critical Phenomena*, edited by C. Domb and J. L. Lebowitz (Academic, New York, 1988), Vol. 12.

[14] R. Kern, G. Le Lay, and J. J. Metois, in *Current Topics in Materials Science*, edited by E. Kaldis (North-Holland, Amsterdam, 1979), Vol. 3.

[15] D. Kashchiev, Surf. Sci. **55**, 477 (1976).

[16] The Xe layers will be polycrystalline and the defect density may be high at 50 K. Clusters that form are attracted to the substrate and each other by the dispersion forces, and they respond to these forces over time [T. R. Ohno, J. C. Patrin, U. S. Ayyala, and J. H. Weaver, Phys. Rev. B **44**, 1891 (1991)]. During Ag deposition and cluster formation, the release of condensation and bond formation energy will cause a certain amount of Xe to sublime, creating defects on the surface. Xe step structures should also be dynamic.